Research Article | Vol. 25, No. 12 | 12 Jun 2017 | OPTICS EXPRESS 13549
Optics EXPRESS

Highly sensitive and selective liquid crystal optical sensor for detection of ammonia

XIAOFANG NIU, YUANBO ZHONG, RUI CHEN, FEI WANG, AND DAN LUO*

Department of Electrical and Electronic Engineering, Southern University of Science and Technology, Xueyuan Road 1088, Nanshan District, Shenzhen, Guangdong, 518055, China
luo.d@sustc.edu.cn

Abstract: Ammonia detection technologies are very important in environment monitoring. However, most existing technologies are complex and expensive, which limit the useful range of real-time application. Here, we propose a highly sensitive and selective optical sensor for detection of ammonia (NH_3) based on liquid crystals (LCs). This optical sensor is realized through the competitive binding between ammonia and liquid crystals on chitosan-Cu^{2+} that decorated on glass substrate. We achieve a broad detection range of ammonia from 50 ppm to 1250 ppm, with a low detection limit of 16.6 ppm. This sensor is low-cost, simple, fast, and highly sensitive and selective for detection of ammonia. The proposal LC sensing method can be a sensitive detection platform for other molecule monitors such as proteins, DNAs and other heavy metal ions by modifying sensing molecules.

OCIS codes: (160.3710) Liquid crystals; (280.4788) Optical sensing and sensors.

References and links

1. N. B. Shustova, A. F. Cozzolino, S. Reineke, M. Baldo, and M. Dincă, "Selective turn-on ammonia sensing enabled by high-temperature fluorescence in metal-organic frameworks with open metal sites," J. Am. Chem. Soc. **135**(36), 13326–13329 (2013).
2. R. J. Huang, Y. Zhang, C. Bozzetti, K. F. Ho, J. J. Cao, Y. Han, K. R. Daellenbach, J. G. Slowik, S. M. Platt, F. Canonaco, P. Zotter, R. Wolf, S. M. Pieber, E. A. Bruns, M. Crippa, G. Ciarelli, A. Piazzalunga, M. Schwikowski, G. Abbaszade, J. Schnelle-Kreis, R. Zimmermann, Z. An, S. Szidat, U. Baltensperger, I. El Haddad, and A. S. H. Prévôt, "High secondary aerosol contribution to particulate pollution during haze events in China," Nature **514**(7521), 218–222 (2014).
3. T. Moise, J. M. Flores, and Y. Rudich, "Optical properties of secondary organic aerosols and their changes by chemical processes," Chem. Rev. **115**(10), 4400–4439 (2015).
4. C. S. Liang, F. K. Duan, K. B. He, and Y. L. Ma, "Review on recent progress in observations, source identifications and countermeasures of PM2.5," Environ. Int. **86**, 150–170 (2016).
5. R. Jalan, F. De Chiara, V. Balasubramaniyan, F. Andreola, V. Khetan, M. Malago, M. Pinzani, R. P. Mookerjee, and K. Rombouts, "Ammonia produces pathological changes in human hepatic stellate cells and is a target for therapy of portal hypertension," J. Hepatol. **64**(4), 823–833 (2016).
6. L. Li, P. Gao, M. Baumgarten, K. Müllen, N. Lu, H. Fuchs, and L. Chi, "High performance field-effect ammonia sensors based on a structured ultrathin organic semiconductor film," Adv. Mater. **25**(25), 3419–3425 (2013).
7. M. G. Campbell, D. Sheberla, S. F. Liu, T. M. Swager, and M. Dincă, "Cu_3(hexaiminotriphenylene)$_2$: an electrically conductive 2D metal-organic framework for chemiresistive sensing," Angew. Chem. Int. Ed. Engl. **54**(14), 4349–4352 (2015).
8. E. Bekyarova, I. Kalinina, M. E. Itkis, L. Beer, N. Cabrera, and R. C. Haddon, "Mechanism of ammonia detection by chemically functionalized single-walled carbon nanotubes: in situ electrical and optical study of gas analyte detection," J. Am. Chem. Soc. **129**(35), 10700–10706 (2007).
9. P. Stamenov, R. Madathil, and J. M. D. Coey, "Dynamic response of ammonia sensors constructed from polyaniline nanofibre films with varying morphology," Sens. Actuators B Chem. **161**(1), 989–999 (2012).
10. R. Ghosh, A. Midya, S. Santra, S. K. Ray, and P. K. Guha, "Chemically reduced graphene oxide for ammonia detection at room temperature," ACS Appl. Mater. Interfaces **5**(15), 7599–7603 (2013).
11. S. Chakraborty, J. T. Gleeson, A. Jakli, and S. Sprunt, "A comparison of short-range molecular order in bent-core and rod-like nematic liquid crystals," Soft Matter **9**(6), 1817–1824 (2013).
12. R. J. Carlton, J. T. Hunter, D. S. Miller, R. Abbasi, P. C. Mushenheim, L. N. Tan, and N. L. Abbott, "Chemical and biological sensing using liquid crystals," Liq. Cryst. Rev. **1**(1), 29–51 (2013).
13. J. Deng, W. Liang, and J. Fang, "Liquid crystal droplet-embedded biopolymer hydrogel sheets for biosensor applications," ACS Appl. Mater. Interfaces **8**(6), 3928–3932 (2016).
14. H. Shahsavan, S. M. Salili, A. Jákli, and B. Zhao, "Smart muscle-driven self-cleaning of biomimetic microstructures from liquid crystal elastomers," Adv. Mater. **27**(43), 6828–6833 (2015).

#294550 https://doi.org/10.1364/OE.25.013549
Journal © 2017 Received 27 Apr 2017; revised 31 May 2017; accepted 31 May 2017; published 6 Jun 2017

Optics EXPRESS

15. A. D. Price and D. K. Schwartz, "DNA hybridization-induced reorientation of liquid crystal anchoring at the nematic liquid crystal/aqueous interface," J. Am. Chem. Soc. **130**(26), 8188–8194 (2008).
16. Q. Liu, Y. Yuan, and I. I. Smalyukh, "Electrically and optically tunable plasmonic guest-host liquid crystals with long-range ordered nanoparticles," Nano Lett. **14**(7), 4071–4077 (2014).
17. S. Yang, C. Wu, H. Tan, Y. Wu, S. Liao, Z. Wu, G. Shen, and R. Yu, "Label-free liquid crystal biosensor based on specific oligonucleotide probes for heavy metal ions," Anal. Chem. **85**(1), 14–18 (2013).
18. S. H. Yoon, K. C. Gupta, J. S. Borah, S. Y. Park, Y. K. Kim, J. H. Lee, and I. K. Kang, "Folate ligand anchored liquid crystal microdroplets emulsion for in vitro detection of KB cancer cells," Langmuir **30**(35), 10668–10677 (2014).
19. A. Hussain, A. S. Pina, and A. C. A. Roque, "Bio-recognition and detection using liquid crystals," Biosens. Bioelectron. **25**(1), 1–8 (2009).
20. R. Manda, V. Dasari, P. Sathyanarayana, M. V. Rasna, P. Paik, and S. Dhara, "Possible enhancement of physical properties of nematic liquid crystals by doping of conducting polymer nanofibres," Appl. Phys. Lett. **103**(103), 141910 (2013).
21. C. H. Chen, Y. C. Lin, H. H. Chang, and A. S. Y. Lee, "Ligand-doped liquid crystal sensor system for detecting mercuric ion in aqueous solutions," Anal. Chem. **87**(8), 4546–4551 (2015).
22. R. R. Shah and N. L. Abbott, "Principles for measurement of chemical exposure based on recognition-driven anchoring transitions in liquid crystals," Science **293**(5533), 1296–1299 (2001).
23. S. S. Sridharamurthy, K. D. Cadwell, and N. L. Abbott, "A microstructure for the detection of vapor-phase analytes based on orientational transitions of liquid crystals," Smart Mater. Struct. **17**(1), 1–4 (2007).
24. K. D. Cadwell, M. E. Alf, and N. L. Abbott, "Infrared spectroscopy of competitive interactions between liquid crystals, metal salts, and dimethyl methylphosphonate at surfaces," J. Phys. Chem. B **110**(51), 26081–26088 (2006).
25. M. L. Bungabong, P. B. Ong, and K. L. Yang, "Using copper perchlorate doped liquid crystals for the detection of organophosphonate vapor," Sens. Actuators B Chem. **148**(2), 420–426 (2010).
26. W. Suginta, P. Khunkaewla, and A. Schulte, "Electrochemical biosensor applications of polysaccharides chitin and chitosan," Chem. Rev. **113**(7), 5458–5479 (2013).
27. X. Kang, J. Wang, H. Wu, I. A. Aksay, J. Liu, and Y. Lin, "Glucose oxidase-graphene-chitosan modified electrode for direct electrochemistry and glucose sensing," Biosens. Bioelectron. **25**(4), 901–905 (2009).
28. E. S. Dragan, D. F. Apopei Loghin, and A. I. Cocarta, "Efficient sorption of Cu2+ by composite chelating sorbents based on potato starch-graft-polyamidoxime embedded in chitosan beads," ACS Appl. Mater. Interfaces **6**(19), 16577–16592 (2014).
29. S. Cui, S. Mao, Z. Wen, J. Chang, Y. Zhang, and J. Chen, "Controllable synthesis of silver nanoparticle-decorated reduced graphene oxide hybrids for ammonia detection," Analyst (Lond.) **138**(10), 2877–2882 (2013).
30. Q. Qi, P. P. Wang, J. Zhao, L. L. Feng, L. J. Zhou, R. F. Xuan, Y. P. Liu, and G. D. Li, "SnO2 nanoparticle-coated In2O3 nanofibers with improved NH3 sensing properties," Sens. Actuators B Chem. **194**, 440–446 (2014).

1. Introduction

Ammonia is one of the most harmful environmental pollutants and a toxic gas to human body [1,2].It has been reported that ammonia contributes to secondary particle formation by reacting with the acidic species such as SnO_2, NO_x, and forming ammonium-containing aerosols [3]. Meanwhile, the concentration of ammonia is a key index for determining air quality through its part in formation of PM2.5 particles in atmosphere and water quality [4,5]. In recent years, several methods to detect ammonia have been developed using such as organic semiconductor [6], metal–organic framework [7], carbon nanotubes [8], polyaniline nanofiber [9] and graphene oxide [10], [10] with limit of detection (LOD) around 100 ppm. However, since modification procedures of these nanometer materials are usually complex and expensive in many practical applications, exploring a fast and cost-effective scheme for detection of ammonia becomes extremely desirable.

Liquid crystal (LC) [11] have attracted much interest due to their unique optical properties and potential applications in various biological [12,13], chemical and material fields [14]. The LCs can be used to transduce molecular events at an interface into macroscopic responses, for example visible with the naked eye. This transduction is extraordinarily sensitive to physical and chemical properties of a bounding interface [15,16]. Several approaches utilizing nematic liquid crystal, e. g. 4-cyano-4'-penthlbiphenyl (5CB), for detection of biomolecule [17–19], polymer chemicals [20] and heavy metal ions [21]. Since Shah and Abbott reported the measurement of chemical exposure based on recognition-driven anchoring transitions in LC, more and more researcher group have developed various methold for detection of vapor-

phase analytes based on LC. Abbott's group also demonstrated the gas sensors using metal salt immobilized liquild crystals which is also useful in interfacial assembly, chemical analysis and biosensor [22–24].

In this letter, for the first time we demonstrate a highly sensitive and selective optical sensor based on liquid crystals for detection of ammonia. This liquid crystals-based chemical sensor is realized through the competitive binding between ammonia and nitrile group of liquid crystals on chitosan-Cu^{2+} that decorated on glass substrate. A broad detection range of ammonia from 50 ppm to 1250 ppm, with a low detection limit of 16.6 ppm, has been achieved. This sensor is low-cost, simple, and fast for detection of ammonia.

Herein we present a generalized strategy for ammonia detection using surface decorated with a metal complexes of chitosan chelate copper ion (CHIT-Cu^{2+}). The design sensor is based on the phenomenon that the LCs with nitrile group (such as 5CB) will be aligned homeotropically due to the coordination complex formed from copper percholorate and nitrile-containing mesogens [25]. The optical image of LCs with homeotropic alignment exhibits a dark appearance when observed in polarizing optical microscope (POM). The substrate of glass slide is functionalized to modify chitosan (CHIT) on it. The CHIT is an aminopolysaccharide that is obtained from deacetylation of chitin, which is one of the most abundant natural polymers [26]. This inexpensive polysaccharide can act as an outstanding adsorbent in transition from chelation to metalion, in which the amino group of the 2-amino-2-deoxy-d-glucose (glucosamine) unit plays an important role [27,28]. By utilizing CHIT together with Cu^{2+} to alignment molecules of 5CB initially, a dark image can be obtained under POM. Besides, (3-aminopropyl)triethoxysilane (APTS) containing amino group is used to functionalize the surface of glass slide and cross-link CHIT through glutaraldehyde (GE).

2. Experiment

2.1 Materials and methods

$Cu(ClO_4)_2$, chitosan (CHIT), glutaraldehyde (GE) 25% (m/v), poly(dimethysiloxane) (PDMS), (3-aminopropyl)triethoxysilane (APTS, 98%) were purchased from Sigma-Aldrich. Microscope slides (Sail Brand) were obtained from Taizhou Dongsheng Glass Co. Ltd., China. 4-n-pentyl-4'-cyanobiphenyl (5CB) was bought from HCCH, Jiangsu Hecheng, China. Sulfuric acid (H_2SO_4, ≥ 96%), and hydrogen peroxide (H_2O_2, 30~35.5%) were purchased from Sinopharm Chemical (Shanghai, China). All the optical images of LC droplets were observed using polarizing optical microscope (Ti 200, Nikon) in transmission mode. In the optical images, the average gray value (G) represented the brightness of birefringent domains, which was evaluated by software ImageJ. A plastic gas box was used to control the concentration of ammonia and relative humidity in experiment. The concentration of ammonia was controlled by mixing ammonia with nitrogen at different volume ratios, and the relative humidity was adjusted by the amount of water vapor adding into the gas box.

2.2 Design principle

The fabrication process of ammonia sensor based on 5CB is illustrated in Fig. 1. A glass slide that was used to decorate metal ion (Cu2 +) was firstly cleaned by a hot piranha solution (H2SO4 (98%): H2O2 (35%) = 3:1) for 30 minutes,then rinsed in copious amount of deionized water, and finally sonicated for another 15 minutes. Next, the glass slide was immersed in the mixture for 10 minutes, which containing 0.3% APTS and 95% acetone. After that, the glass slide was dried under a stream of nitrogen (N2) and heated at 40 oC for at least 3 hours. As a result, the surface of glass slide was modified with amidogen, after which 1% glutaraldehyde (GE) was dip-coated on the slide and stood for 1 hour. Afterwards, 0.5% CHIT was mixed with 65 mmol/L Cu(ClO4)2 for 10 minutes and then deposited on the glass slide by spin coating. The copper solution was dispensed on the substrate twice: the speed and time are 400 rpm and 20 s for the first coating and 850 rpm and 30 s for the second coating,

respectively. Finally, the prepared slide was heated in a drying oven at 110 °C for 90 minutes and then stored at room temperature. In this situation, the CHIT-Cu2 + was effectively immobilized onto the glass slide by a strong cross-link between GE and CHIT. A TEM grid was placed onto the glass slide that decorated with Cu2 + . The injected 5CB molecules in the grid formed a LC film with thickness around 10 μm. The initial orientation of 5CB molecules were perpendicularly aligned on the surface decorated with CHIT-Cu2 + , which was the complexation of the nitrile groups (–CN) of 5CB with Cu2 + [22]. A LC cell was assembled by the metal ion decorated slide and another a glass slide covered. Poly(dimethysiloxane) (PDMS) walls with thickness of 5 mm was fabricated on the slide of the LC cell, where two pin holes was drilled on the wall for vapor sampling.

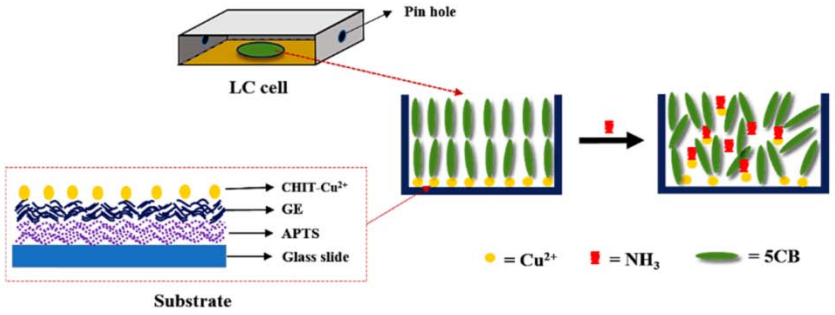

Fig. 1. Fabrication process of LC based optical sensor for ammonia detection.

When the ammonia was added, a competitive reaction between ammonia and 5CB would result in preferential binding of ammonia to the Cu^{2+}. The nitrile groups of the LCs from the coordination interaction with the Cu^{2+} was replaced by the complex of $Cu(NH_3)_4^{2+}$. This change in interfacial interaction leaded to the re-alignment of LCs from homeotropic state to random state with an associated increase in the amount of light transmitted through the LC film observed under POM.

2.3 Characterization

To confirm that the 5CB was successfully anchored on the substrate, a control experiment was implemented. Here, one group of glass slide was modified with 200 mmol/L $Cu(ClO_4)_2$ and 0.5% CHIT, which was critical to the decoration of CHIT-Cu^{2+} on glass slide, and another group of glass slide was only modified with 0.5% CHIT. Both of them were then assembled to LC cells for ammonia detection. Figure 2 shows the observed optical images under POM for two groups exposed to 500 ppm ammonia. The group that was modified with $Cu(ClO_4)_2$ showed a uniform dark region when viewed under POM (Fig. 2(a)), indicating the LC molecules aligned perpendicularly on the glass substrate. The interaction between Cu^{2+} and –CN of 5CB resulted in a homeotropic anchoring. In contrast, another group that wasn't modified with $Cu(ClO_4)_2$ was bright when viewed under POM (Fig. 2(b)), indicating the LC molecules aligned randomly on the substrate without CHIT-Cu^{2+} decoration. Therefore, based on aforementioned experiment, we could confirm that the CHIT-Cu^{2+} exhibited a good performance for anchoring 5CB on the substrate with homeotropic alignment.

Optics EXPRESS

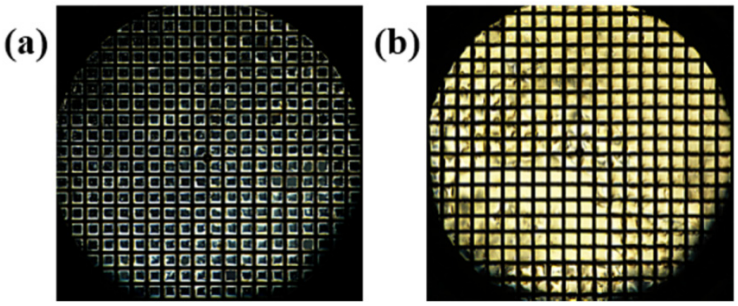

Fig. 2. Optical appearances viewed under crossed polarizers of LC cells decorated (a) with Cu^{2+} and (b) without Cu^{2+}.

2.4 Optimization of experiment conditions

In order to identify the transition time of LC molecules from homeotropic to random alignment, corresponding to optical images changing from dark to bright after exposure in ammonia, further testing was conducted in the detection process. Without ammonia, the observed optical image was dark, as shown in Fig. 3(a). When the sensor was exposed to 800 ppm of ammonia, the optical image quickly transformed from dark to bright with increase of exposure time, and the optical image finally reached a stable state when the exposure time increased to 100 s. Figure 3(b)-3(f) shows the optical images observed under POM of LC based sensor exposed to ammonia for (b) 10 s, (c) 25 s, (d) 50 s, (e) 75 s, and (f) 100 s, respectively. As the image remained stable after ammonia exposure for 100 s, thus 100 s was selected as the optimal reaction time for detection 800 ppm of ammonia in our experiment.

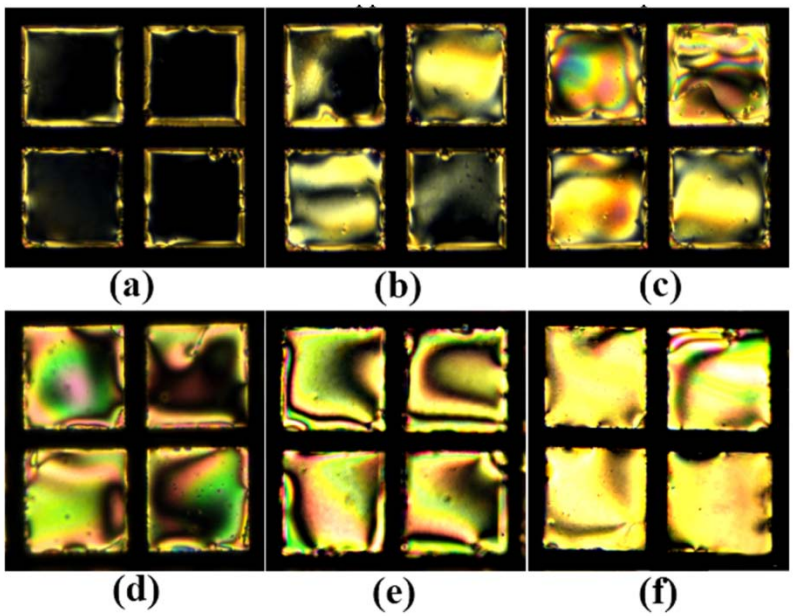

Fig. 3. Optical images of LC based optical sensor exposed in ammonia for (a) 0 s (b) 10 s, (c) 25 s, (d) 50 s, (e) 75 s, and (f) 100 s.

The concentration of Cu^{2+} used in fabrication process that decorated on glass slide would have significant influence on the stability of the homeotropic alignment formed by LC. Figure 4(a) shows the average gray value versus the time with different concentration of Cu^{2+}. The average gray value was estimated from the optical image observed under POM. The sample

decorated with high concentration of Cu^{2+} exhibited good anchoring strength for LC molecules initially. At the beginning, the obtained average gray values varied from 62% to more than 80%, when the concentration of Cu^{2+} varied from 50 to 350 mmol/L. With the increase of time, the average gray values declined sharply for all concentrations except the 175 mmol/L. The reason might be explained following: for high concentration of 350 and 250 mmol/L, the Cu^{2+} was over-saturated initially and dissolved in 5CB with time increased, resulting in a fast decay of average gray value. On the contrary, for low Cu^{2+} concentration of 100 and 50 mmol/L, the Cu^{2+} was too little to bind most of the 5CB molecules initially and then dissolved in 5CB with time increased, thus leaded to random alignment of 5CB hence decay of average gray value. For the concentration of 175 mmol/L, the sample exhibited a good stability, and the average gray value decayed from 83% to 76% in 90 hours, indicating the anchoring ability was optimal here. Therefore, the concentration of 175 mmol/L was used in the experiment.

The response of average gray value at different relative humidities of 30%, 45%, 60%, 75% and 90% was shown in Fig. 4(b). We could see that the average gray value increased with the increase of relative humidity and reached its maxima when the relative humidity was 60%, beyond which the average gray value started to decrease. High humidity beyond 60% may have negative effect on CHIT-Cu^{2+} immobilization on the surface of glass substrate, therefore the 60% of relative humidity was selected in this experiment.

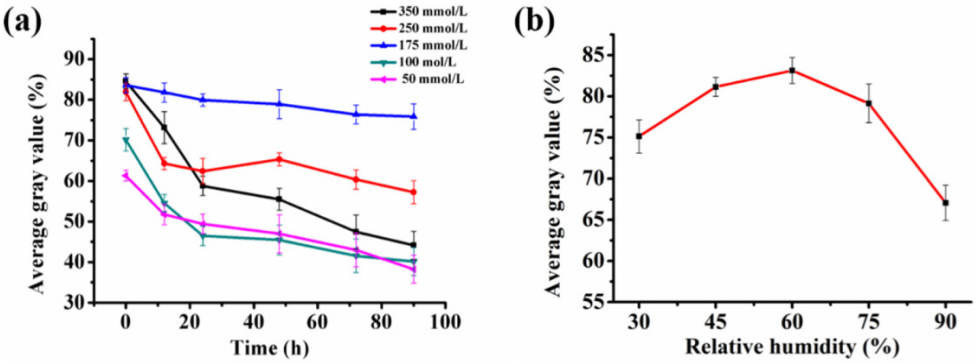

Fig. 4. Response of average gray value in different condition: (a) with increase of time from 0 to 90 h in the presence of 50, 100, 175, 250 and 350 mmol/L of Cu^{2+}; (b) different relative humidity from 30% to 90% in the system.

3. Results and discussion

3.1 Performance of the sensing method

The LC sensor limit of detection for ammonia detection is a critical parameter that determines the quality of sensor. The LC sensor limit of detection tested through measuring the detection limit of the LC sensor for ammonia, while keeping the exposure time fixed at 100 s. Figure 5 shows the response curve and the optical images of LC sensor (three groups of samples) exposed in different concentrations of ammonia such as 50 ppm, 100 ppm, 250 ppm, 500 ppm, 750 ppm, 1000 ppm, and 1250 ppm. Before the LC cell was exposed in ammonia, the average gray value was expressed in G_0. Moreover, the relative gray values reduction with the expression $(G_0- G)/G_0$ showed a dynamic range for ammonia covering from 50 ppm to 1250 ppm with a detection limit of 16.6 ppm using 3σ criteria, which was better than the results reported by Cui and Qi using nanoparticle to sense ammonia [29,30]. With increase of ammonia concentration, the observed brightness of optical image increases. The higher concentration of ammonia exposed to the LC sensor, the more competitive binding reactions of ammonia on the Cu^{2+} happened, which leaded to more random orientations of LC molecules and more brightness in optical image.

Optics EXPRESS

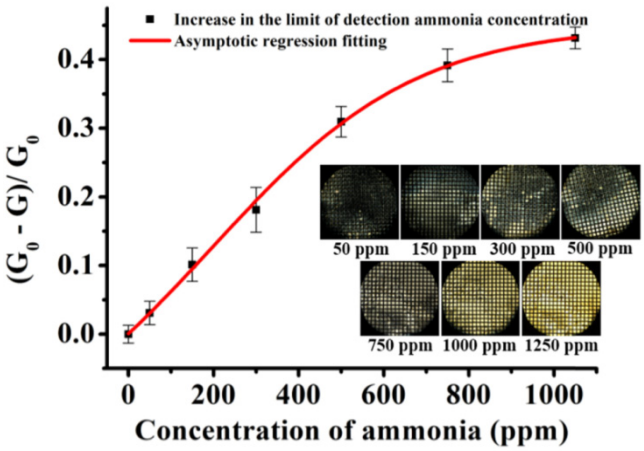

Fig. 5. Response curve and optical images of the sensor for ammonia after it exposed in different concentration: 50 ppm, 100 ppm, 250 ppm, 500 ppm, 750 ppm, 1000 ppm and 1250 ppm.

3.2 Selectivity of LC sensor

To demonstrate the specificity of the LC sensor for ammonia, 800 ppm H_2S, 800 ppm SO_2, 800 ppm Cl_2, 800 ppm CO_2, 800 ppm CO and 250 ppm NH_3 were tested. Figure 6 shows that the LC sensor has negligible response to H_2S, SO_2, Cl_2, CO_2 and CO under the same conditions, illustrating that the LC sensor has a high selectivity for ammonia.

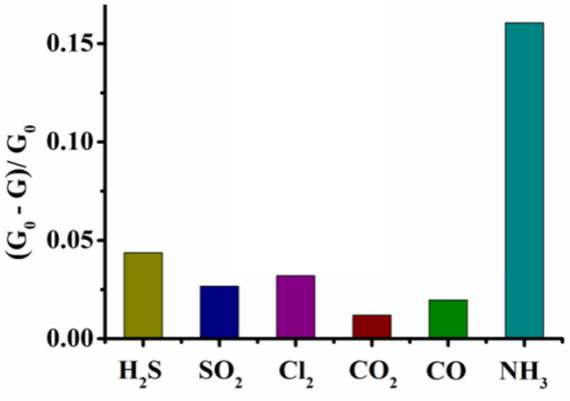

Fig. 6. The selectivity of LC based optical sensor exposed in different gases: 800 ppm H_2S, 800 ppm SO_2, 800 ppm Cl_2, 800 ppm CO_2, 800 ppm CO and 250 ppm NH_3.

3.3 Study of Cu^{2+} dissolved in LC

An experiment was carried on to investigate whether Cu^{2+} was dissolved in LC. When the Cu^{2+} without CHIT was spin-coated directly on the glass substrate, the Cu^{2+} was dissolved in LC because it couldn't be immobilized on the substrate without CHIT, and the corresponding POM image was shown in Fig. 7(a). Here two samples are fully exposed in ammonia to make sure sufficient response. The dissolved Cu^{2+} disturbed the orientation of LC molecules randomly and leaded to a colorful optical image. In contrast, when the Cu^{2+} with CHIT was spin-coated on the glass substrate, the Cu^{2+} was not dissolved in LC because it could be immobilized on the substrate. The obtained optical image of Fig. 7(a) isn't uniform and quite different from the previously situation, while Fig. 7(b) shows a uniform homeotropic in the same condition.

Optics EXPRESS

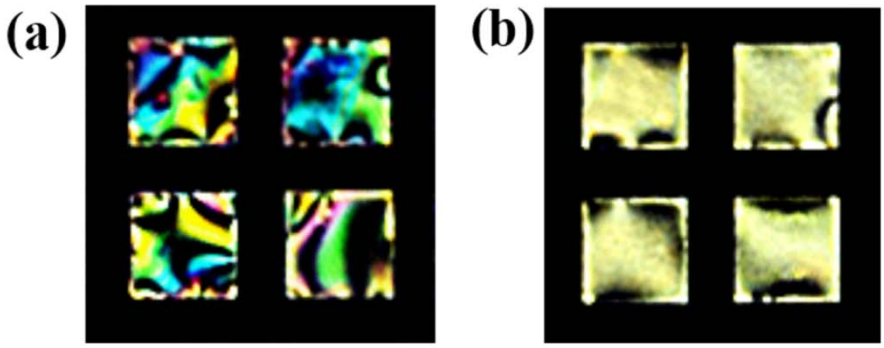

Fig. 7. Optical images of the Cu^{2+} (a) dissolved in LC and (b) undissolved in LC.

4. Conclusion

In conclusion, we demonstrate an ammonia sensor based on liquid crystals. This liquid crystals-based chemical sensor is realized through the competitive binding between ammonia and nitrile group of liquid crystals on Cu^{2+} that could induce the alignment of nematic liquid crystal 5CB initially. The change on alignment of 5CB can transduce in optical image under polarizing optical microscope. The limit of detection and stability of LC sensor have been studied experimentally. The resultant sensor is low cost, simple and fast for sensing ammonia. The proposal method can be extended to detect proteins, DNAs and other heavy metal ions in chemical and biological applications.

Funding

National Natural Science Foundation of China (NSFC) (61405088, and 11574130); Shenzhen Science and Technology Innovation Council (JCYJ20150601155130435, JCYJ20160226192528793, JCYJ20150930160634263, and KQTD2015071710313656).